JOURNAL OF COMPUTATIONAL PHYSICS 79, 167–183 (1988)

On Modulational Instabilities in Discretisations of the Korteweg–de Vries Equation

D. M. SLOAN

Department of Mathematics, University of Strathclyde, Glasgow G1 1XH, Scotland

Received December 29, 1986; revised November 13, 1987

W. L. Briggs, A. C. Newell, and T. Sarie (*J. Comput. Phys.* **51**, 83 (1983)) have studied nonlinear instabilities in discretisations of the equation $u_t + (u+U)\,u_x = 0$, where U is a constant. They demonstrated that solutions of leap-frog discretisations of this equation could be destabilised by a dynamical process which can localise noise on the spatial grid. D. M. Sloan and A. R. Mitchell (*J. Comput. Phys.* **67** (1986)) examined these instabilities by considering perturbations of the basic solution which take the form of side-band Fourier modes. Here this latter work is extended to cover analogous discretisations of the Korteweg–de Vries equation.

1. INTRODUCTION

A recent paper by Briggs, Newell, and Sarie [2] described a mechanism which produces instabilities in nonlinear partial difference equations. Their ideas were illustrated by considering leap-frog discretisations of the nonlinear equation

$$u_t + (u+U)\,u_x = 0, \tag{1.1}$$

in which U is a constant, and basic solutions were considered which satisfy the unit periodic boundary condition

$$u(x+1, t) = u(x, t). \tag{1.2}$$

To solve the problem in $0 \leqslant x \leqslant 1$ this region was discretised using a grid size $h = 1/J$, where J is an even integer. The basic solutions used were those which contain a small number, say N, Fourier modes of the form $\exp(2\pi ijp/J)$, $j = 0, 1, \ldots, J$, where p is an integer satisfying $|p| \leqslant J/2$. U in (1.1) may be regarded as a constant solution of the inviscid Burgers equation, and the periodic solutions are then perturbations about this constant state. If the constant state is characterised by a parameter α and if the energy in the perturbation is characterised by a parameter E, it is possible to find regions in (α, E) space within which an N-mode basic solution appears to be stable. Briggs *et al.* [2] have shown that the basic solutions are actually destabilised by long wavelength disturbances. As the instability grows the

0021-9991/88 $3.00

basic solution is modulated and Fourier side-bands of the basic N modes draw energy from these basic modes. This dynamical process concentrates energy at certain locations on the spatial grid and the solution quickly becomes unbounded.

Sloan and Mitchell [7] examined the same model using an approach related to that adopted by Benjamin and Feir [1] in their analysis of wavetrain instabilities in deep water. Numerical experiments performed by Sloan and Mitchell [7] confirmed that the side-band growth is related to the leap-frog discretisation of the time variable. They also indicated that instabilities develop on a long time scale. This notion has subsequently been developed by Cloot and Herbst [3] who performed a multiple scales analysis to show that the instabilities are caused by a resonance effect introduced by the discretisations. Their analysis supports the observations made by Briggs *et al.* [2] and by Sloan and Mitchell [7].

In this note the work by Sloan and Mitchell [7] is extended to the Korteweg–de Vries (KdV) equation. We consider the N-mode solution for $N=1$ only. Experiments show that the dispersive term can have a stabilising or a destabilising effect, depending on the circumstances. For example, when the constant U in Eq. (1.1) is zero the 1-mode solution is always unstable. This result was first obtained by Fornberg [5] and discussed further by Sloan and Mitchell [7]. Here it is shown that stable 1-mode perturbations about the zero state are possible for the KdV equation. Furthermore, Sloan and Mitchell [7] observed no side-band growth in the semi-discrete form of (1.1), and their observations were confirmed by the multiple scales analysis of Cloot and Herbst [3]. For the KdV equation, however, it is shown here that the semi-discrete system may exhibit side-band growth.

2. 1-Mode Equations

2.1. *Difference Equations*

Here we consider the perturbed KdV equation

$$u_t + (u+U)\,u_x + \varepsilon u_{xxx} = 0, \tag{2.1}$$

where U and ε are constants and $u(x, t)$ satisfies the periodicity condition (1.2). A leap-frog discretisation on a grid with time step k and space step $h = 1/J$ is

$$U_j^{n+1} - U_j^{n-1} + \frac{\theta\gamma}{2}\left[(U_{j+1}^n)^2 - (U_{j-1}^n)^2\right] + \left[(1-\theta)\,\gamma U_j^n + \alpha\right]\left[U_{j+1}^n - U_{j-1}^n\right] + \beta\left[U_{j+2}^n - 2U_{j+1}^n + 2U_{j-1}^n - U_{j-2}^n\right] = 0, \tag{2.2}$$

where U_j^n approximates $u(jh, nk)$, $\gamma = k/h$, $\alpha = \gamma U$, $\beta = \gamma\varepsilon/h^2$ and the real parameter θ satisfies the constraint $0 \leqslant \theta \leqslant 1$. Scheme (2.2) is used for $j = 1, 2, \ldots, J$, $n \geqslant 1$, and the periodicity condition is imposed in the form

$$U_{J+1}^{n+1} = U_1^{n+1},\ U_{J+2}^{n+1} = U_2^{n+1},\ U_0^{n+1} = U_J^{n+1},\ U_{-1}^{n+1} = U_{J-1}^{n+1}. \tag{2.3}$$

Equations (2.2) and (2.3) satisfy the invariance conditions given in Sloan and Mitchell [7]: in particular, if $\theta = \frac{2}{3}$, we have

$$\sum_{j=1}^{J} U_j^n U_j^{n+1} = \text{constant}, \qquad n \geqslant 0. \tag{2.4}$$

This near-conservation condition suggests that $\frac{2}{3}$ might be an appropriate value for the parameter θ.

It is readily shown that $U_j^n = \xi^n \exp(2\pi ijp/J)$, $0 \leqslant p \leqslant J/2$ is a stable solution of the linear portion of (2.2) if

$$|\zeta| = (\sin \eta)\, |\alpha + 2\,\beta(\cos \eta - 1)| \leqslant 1, \text{ where } \eta = 2\pi p/J. \tag{2.5}$$

ξ^n may then be written as $\exp(-in\phi)$, and $\phi \in \mathbb{R}$ assumes one of the values

$$\phi_1 = \arctan\left[\frac{\zeta}{\sqrt{(1-\zeta^2)}}\right], \qquad \phi_2 = \pi - \phi_1. \tag{2.6}$$

It may be shown that a convenient sufficient condition for linear stability, derived from (2.5), is that

$$\max\left\{\alpha, \frac{3\sqrt{3}}{2}\beta\right\} \leqslant 1, \tag{2.7}$$

where α and β are assumed to be non-negative. This condition has been considered by Sanz-Serna [6].

2.2. 1-*Mode Equations and Their Stability*

The semi-discrete form of (2.1) may be written as

$$\dot{U}_j + \frac{\theta}{4h}[(U_{j+1})^2 - (U_{j-1})^2] + \frac{1}{2h}[(1-\theta)\,U_j + U][U_{j+1} - U_{j-1}]$$

$$+ \frac{\varepsilon}{2h^3}[U_{j+2} - 2U_{j+1} + 2U_{j-1} - U_{j-2}] = 0, \tag{2.8}$$

where $U_j(t)$ is an approximation to $u(jh, t)$ and the dot denotes differentiation with respect to t. The 1-mode solution of (2.8) has the form

$$U_j(t) = A(t)\exp(2\pi ij/3) + A^*(t)\exp(-2\pi ij/3), \tag{2.9}$$

where $A(t)$ and its complex conjugate $A^*(t)$ satisfy

$$\dot{A}(t) + \frac{i\sqrt{3}}{2h}\left[U - \frac{3\varepsilon}{h^2}\right]A(t) = \frac{i\sqrt{3}}{4h}(2 - 3\theta)\,A^{*2}(t). \tag{2.10}$$

A midpoint rule discretisation of (2.10) gives the difference equation

$$A(n+1)-A(n-1)+i\sqrt{3}v\,A(n)=\frac{i\sqrt{3}}{2}\gamma(2-3\theta)\,A^{*2}(n), \tag{2.11}$$

where $v=\alpha-3\beta$ and $A(n)$ is an approximation to $A(t)$ at $t=nk$. This is an extension of the 1-mode system used by Briggs *et al.* [2] and Sloan and Mitchell [7] for the inviscid Burgers equation.

A precise description of the nonlinear stability threshold was given by Sloan and Mitchell [7] for the semi-discrete 1-mode system. The analysis is readily applied to the KdV equation. If $A(t)=X(t)+iY(t)$, Eq. (2.10) may be written as a pair of real, nonlinear equations in X and Y. The integral curve pattern of these equations is similar to that given as Fig. 1 in [7], and there it is shown that the system is stable if the initial value of $A\equiv(X, Y)$ is strictly inside a specified triangle PQR in the (X, Y) plane. The coordinates of P, Q, and R are $(N, 0)$ and $(-N/2, \pm\sqrt{3}N/2)$, where

$$N=\left(U-\frac{3\varepsilon}{h^2}\right)\Big/\left(1-\frac{3\theta}{2}\right). \tag{2.12}$$

Stability constraints have been considered fully in Sloan and Mitchell [7] for the case $\varepsilon=0$. Here we need only mention modifications introduced by the introduction of non-zero ε. Note also that the stability analysis for the semi-discrete system gives guidance concerning the stability region for the fully discrete system (2.11). An essential requirement in the latter case is that the discrete approximations $A(0)$, $A(1)$, $A(2)$, ... should remain inside the aforementioned triangle PQR. As in Sloan and Mitchell [7] the stability of (2.11) was investigated by solving the difference equation using starting values $A(0)=A(1)=\sigma(1+i)$, where σ is a positive constant and (σ, σ) is in triangle PQR. The maximum norm of the initial data is

$$E=\sigma(\sqrt{3}+1) \tag{2.13}$$

and this is used as a measure of the initial energy in the 1-mode solution. To obtain the stability threshold for given α and β, Eq. (2.11) was integrated using increasing values of E until we found the maximum E at which the solution remained bounded over 2×10^4 time steps.

Note that any comments on the nonlinear stability of (2.11) should be restricted to the parameter range $|\alpha-3\beta|\leqslant 2/\sqrt{3}$, within which (2.11) is linearly stable. This stability limit is precise at $\theta=\frac{2}{3}$. In general, (2.11) becomes unstable at lower values of $|\alpha-3\beta|$ and experiments by Sloan and Mitchell [7] have shown, for example, that at $\theta=0$ stability holds only if

$$|\alpha-3\beta|<1. \tag{2.14}$$

It is readily shown, using the stability triangle defined at (2.12), that the semi-discrete system (2.10) is nonlinearly stable under the condition

$$\begin{aligned} E &< N, && \text{if} \quad N > 0; \\ E &< \frac{(1+\sqrt{3})}{2}(-N), && \text{if} \quad N < 0. \end{aligned} \tag{2.15}$$

Here N is conveniently defined as $N = (\alpha - 3\beta)/1 - \frac{3}{2}\theta) = \nu/(1 - \frac{3}{2}\theta)$, if we assume, as in Sloan and Mitchell [7], that $\gamma = k/h = 1$.

Inequalities (2.15) enable us to determine the effects of variations in θ, α, or β on the stability threshold for the 1-mode semi-discrete system. If $\nu > 0$, for example, the

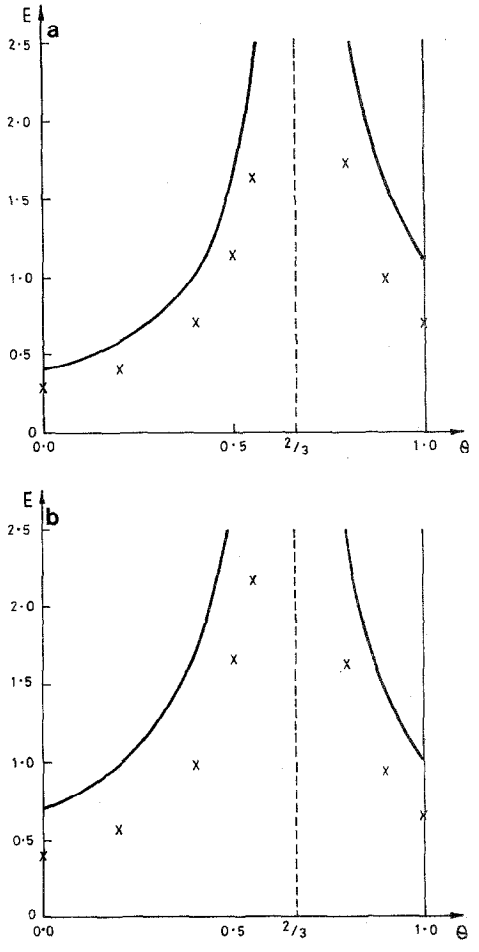

FIG. 1. Variation of the stability threshold with θ for the 1-mode system. Unbroken curve gives semi-discrete threshold and × gives fully discrete threshold. (a) corresponds to $\alpha = 1$, $\beta = 0.2$ ($\nu > 0$) and (b) corresponds to $\alpha = 1$, $\beta = 0.5$ ($\nu < 0$).

threshold energy is v at $\theta = 0$ and $(1+\sqrt{3})\,v$ at $\theta = 1$: it rises from each of these values to infinity as θ approaches the value $\frac{2}{3}$. If $v < 0$ the values at $\theta = 0$ and $\theta = 1$ are, respectively, $(1+\sqrt{3})(-v)/2$ and $-2v$ and from each of these it rises as θ approaches $\frac{2}{3}$. The unbroken curves in Fig. 1 show the variation with θ of the stability threshold for the 1-mode semi-discrete system. The profile in Fig. 1a corresponds to parameter values $\alpha = 1$, $\beta = 0.2$ and it shows the variation when $v > 0$. Figure 1b corresponds to $\alpha = 1$, $\beta = 0.5$ and it shows the situation when $v < 0$. The variation of the stability threshold with θ was checked numerically for the fully- discrete system (2.11). The profile was found to be qualitatively similar to the semi-discrete profile, but the fully discrete profile is lower. Fully discrete threshold values are marked $\times$ in Figs. 1a, b for the values of α and β specified in the semi-discrete case. Note, for example, that at $\alpha = 1$, $\beta = 0.2$ the semi-discrete and fully discrete threshold values are 0.4 and 0.28, respectively, at $\theta = 0$.

In the semi-discrete case the variation of the threshold profile with α is particularly simple. The unbroken curves in Figs. 2a and b show the semi-discrete

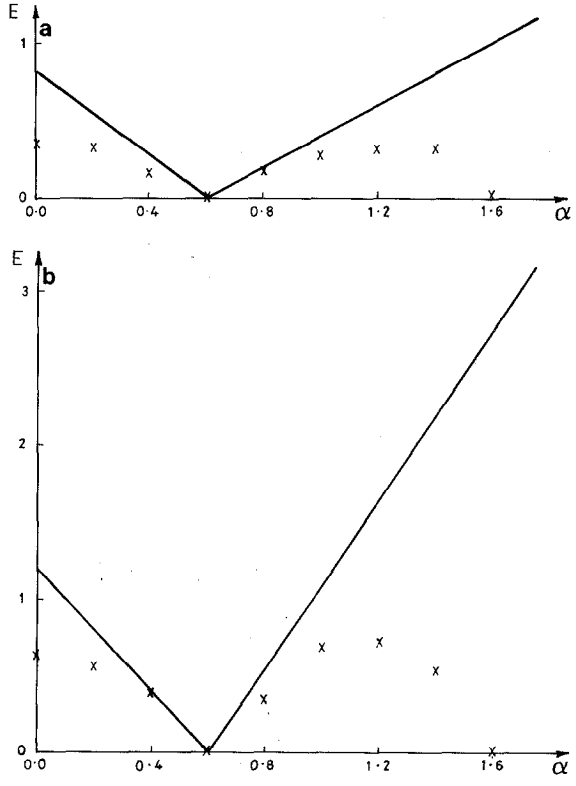

FIG. 2. Variation of the stability threshold with α for the 1-mode system. Unbroken curve gives semi-discrete threshold and $\times$ gives fully discrete threshold. (a) corresponds to $\theta = 0$, $\beta = 0.2$ and (b) corresponds to $\theta = 1$, $\beta = 0.2$.

profiles for $\theta = 0$ and $\theta = 1$, respectively. In each case $\beta = 0.2$ and the variation with α is shown for $0 \leqslant \alpha \leqslant 3\beta + 2/\sqrt{3}$ $(= \alpha_m)$. One notes that if $\beta \in (0, 2/3\sqrt{3})$ and α is restricted to this range then $|\alpha - 3\beta| \leqslant 2/\sqrt{3}$ and (2.11) is linearly stable. The figures show that the semi-discrete threshold is a piecewise linear function of α, with the value zero at $\alpha = 3\beta$. Numerical experiments with Eq. (2.11) have shown that the threshold profile in the fully discrete case is qualitatively similar as α increases from zero to the value 3β. As α increases beyond 3β, however, the threshold rises before it falls rapidly to zero. This deviation from the behaviour of the semi-discrete

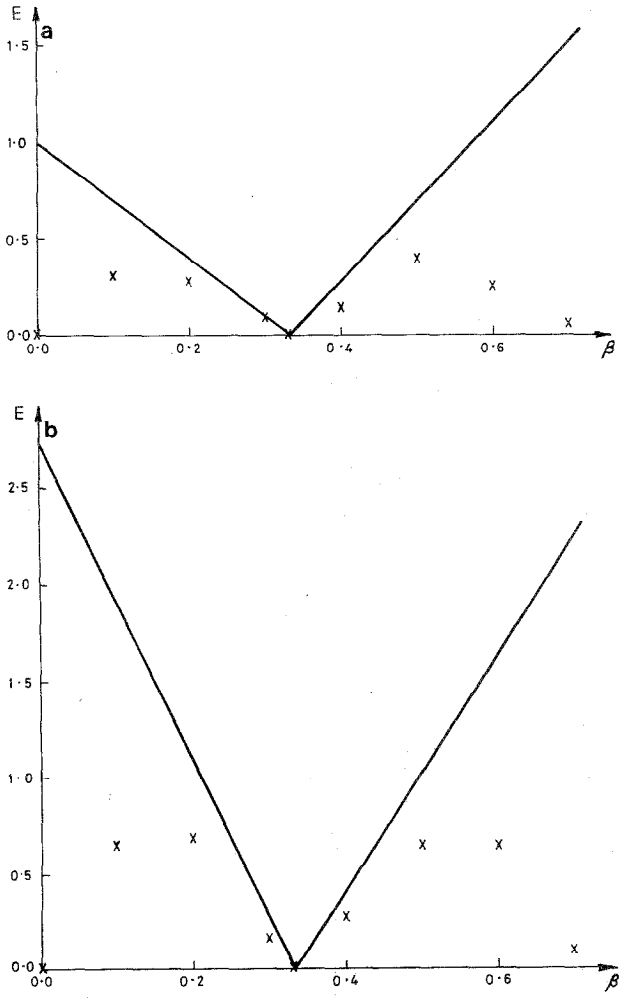

FIG. 3. Variation of the stability threshold with β for the 1-mode system. Unbroken curve gives semi-discrete threshold and × gives fully discrete threshold. (a) corresponds to $\theta = 0$, $\alpha = 1$ and (b) corresponds to $\theta = 1$, $\alpha = 1$.

profile occurs as the stability limit (2.14) is approached. For example, with $\theta = 0$ and $\beta = 0.2$ the threshold falls from 0.32 to zero as α increases from 1.4 to 1.6. Fully discrete values are marked $\times$ in Figs. 2a, b.

The piecewise linear variation of the semi-discrete threshold with β is given by the unbroken curves in Fig. 3. The cases $\theta = 0$ and $\theta = 1$ are displayed in Figs. 3a and b, respectively: in each case $\alpha = 1$ $(\alpha < 2/\sqrt{3})$ and β is in the range $0 \leqslant \beta \leqslant \alpha/3 + 2/3\sqrt{3}$ $(= \beta_m)$. The fully discrete values are seen to fall to zero as the limit (2.14) is approached. Note that the more restrictive condition (2.7) is violated in Figs. 2 and 3.

The stability of the 1-mode system for the KdV equation differs in one significant way from that of the inviscid Burgers equation. For the latter, any perturbation about zero with spatial frequency $3h$ is unstable: this has been discussed by Fornberg [5], among others. For the KdV equation we see that at $\alpha = 0$ and $\theta = 0$, for example, the semi-discrete 1-mode system is stable if $E < 3\beta(1 + \sqrt{3})/2$. This stability at $\alpha = 0$ holds for the fully discrete equation (2.11), as shown in Fig. 2a, and also for the partial difference scheme (2.2) and (2.3). The latter was integrated using $\theta = 0$, $\gamma = 1$, $\beta = 0.2$, and $J = 60$, with initial conditions given by (2.9) and $A(0) = A(1) = \sigma(1 + i)$. The limiting threshold energy was found to be in the interval $E \in (0.35, 0.36)$. The scheme has therefore been stabilised to $3h$ perturbations about zero by the dispersive term.

3. Side-Band Equations

As shown in Sloan and Mitchell [7], if the 1-mode solution of (2.8) is perturbed by Fourier components close to the fundamental the perturbed solution to first order is

$$U_j = Ae^{i\rho j} + A^* e^{-i\rho j} + a_- e^{i(\rho-\delta)j} + a_-^* e^{-i(\rho-\delta)j} + a_+ e^{i(\rho+\delta)j} + a_+^* e^{-i(\rho+\delta)j} + be^{i\delta j} + b^* e^{-i\delta j}, \tag{3.1}$$

where each of the coefficients depends on t, and $\rho = 2\pi/3$, $\delta J = 2\pi\mu$, with μ typically a small positive integer. If we substitute (3.1) into (2.8) and ignore squares of small terms such as $a_+(t)$, we obtain the linearised system

$$\begin{aligned} \dot{a}_- + iF(\delta)\, a_- + i(K(\delta)\, Ab^* - M(\delta)\, A^* a_+^*) &= 0, \\ \dot{a}_+ + iF(-\delta)\, a_+ + i(K(-\delta)\, Ab - M(-\delta)\, A^* a_-^*) &= 0, \\ \dot{b} + iL(\delta)\, b + i(N(\delta)\, Aa_-^* - N(-\delta)\, A^* a_+) &= 0, \end{aligned} \tag{3.2}$$

where

$$F(\delta)=\frac{1}{2h}(\sqrt{3}\cos\delta+\sin\delta)\left[U-(2+\cos\delta-\sqrt{3}\sin\delta)\frac{\varepsilon}{h^2}\right],$$

$$K(\delta)=\frac{1}{2h}[\sqrt{3}-2\sin\delta+\theta(3\sin\delta+\sqrt{3}\cos\delta-\sqrt{3})],$$

$$M(\delta)=\frac{1}{2h}[\sqrt{3}+\sqrt{3}\cos\delta-\sin\delta-\sqrt{3}\,\theta(2\cos\delta+1)],$$

$$N(\delta)=\frac{1}{2h}[\sqrt{3}-\sqrt{3}\cos\delta-\sin\delta+\theta(3\sin\delta+\sqrt{3}\cos\delta-\sqrt{3})]$$

and

$$L(\delta)=\frac{1}{h}(\sin\delta)\left[U-2(1-\cos\delta)\frac{\varepsilon}{h^2}\right].$$

Any growth of the side-band perturbations introduces a modulation which replaces the constant envelope of the basic solution by a periodic function of wavelength $1/\mu$. Nonlinear interactions introduce additional Fourier modes, of course, and the clarity of the modulation will depend on the energy distribution over the Fourier modes. This effect is clearly noticed on Figs. 5c and 7c of Sloan and Mitchell [7] which show, respectively, a 1-mode and 2-mode solution of (2.8) with side-band perturbations. In the 1-mode case, where the modulation is not distinct, only 18.8% of the total energy remains in the basic solution and side-band modes represented by (3.1). In the 2-mode case, however, where modulation is distinct, 95.1% of the total energy remains in the basic solution and side-band modes. Note that the system is not conservative and the total energy is not time-independent.

The growth in modulations in a perturbed 1-mode basic solution of the semi-discrete system (2.8) will depend on the growth of solutions of (3.2). Any modulational instability will develop on a slow time scale, and the presence of different time scales may be observed if $A(t)$ is given by the linear part of (2.10) as

$$A(t)=a_0\,e^{-i\omega t}, \tag{3.3}$$

where $\omega=\sqrt{3}\,(U-3\varepsilon/h^2)/2h$. If we let $h\to 0$ with μ fixed, $\theta=0$, and $\varepsilon=O(h^2)$, the limiting form of (3.2) is

$$\begin{aligned}
&\dot{a}_- + i\omega a_- + \frac{\sqrt{3}\,i}{2h}(a_0\,b^*\,e^{-i\omega t}-2a_0^*\,a_+^*\,e^{i\omega t})=0,\\
&\dot{a}_+ + i\omega a_+ + \frac{\sqrt{3}i}{2h}(a_0\,be^{-i\omega t}-2a_0^*\,a_-^*\,e^{i\omega t})=0,\\
&\dot{b}+i\Omega b-\pi\mu i(a_0 a_-^*\,e^{-i\omega t}+a_0^*\,a_+\,e^{i\omega t})=0,
\end{aligned} \tag{3.4}$$

where $\Omega = 2\pi\mu U$. It may now be seen that the solution of (3.4), and hence of (3.2), evolves on a fast time scale $T = \omega t$ and also on a slow time scale $\tau = \Omega t$. Additional time scales may be introduced by making assumptions concerning the orders of magnitude of $A(t)$ and ε in relation to h. The analysis of this problem is now being considered by the author and it will be reported in due course.

To check for modulational instabilities in the inviscid Burgers equation (1.1) Sloan and Mitchell [7] integrated the analogue of system (3.2) over a large range of the slow time scale. Their experiments suggested that if the initial conditions on the basic 1-mode solution satisfy the stability condition (2.15) then the semi-discrete system corresponding to (1.1) does not permit side-band growth. Cloot and Herbst [3] have subsequently used a multiple scales analysis appropriate to a weakly nonlinear system to support the observations of Sloan and Mitchell [7]. It is of some interest, therefore, to examine the possibility of side-band growth for the semi-discretisation (2.8) of the KdV equation. In particular, one is interested in determining whether or not the presence of non-zero ε alters the stability properties.

We used an accurate integrator to solve (3.2) and (2.10) with parameter values $J = 120$, $\mu = 3$, $\theta = 0$, $U = 0.6$, and several values of ε in the range $0 \leqslant \varepsilon < 7.0 \times 10^{-6}$. Initial conditions were chosen as $A(0) = \sigma(1+i)$, $a_+(0) = 0.5 \times 10^{-4}(1+i)$, $a_-(0) = b(0) = 0$, with $E = 0.2$ and σ given in terms of E by (2.13). The basic solution corresponds to Fourier mode number 40 and the initial perturbation is in mode number 43. It is readily seen that for the given parameter values the basic solution is stable according to (2.15) and any nonlinear instability must therefore be due to the presence of the perturbation.

Figures 4a, b, and c show the variations of the real parts of a_+ and b with time for $\varepsilon = 0$, 4.5×10^{-6}, and 6.5×10^{-6}, respectively. The solutions are shown for an interval $0 \leqslant t \leqslant T$, where T has been chosen so that each figure shows approximately the same number of high frequency oscillations. The values of T in Figs. 4a, b, and c are 4.4, 6.3, and 7.7, respectively, and the figures have been scaled so that $\max_{0 \leqslant t \leqslant T} \{|a_+(t)|, |b(t)|\} = 1$. The high frequency oscillation represents the oscillation in a_+ with period close to $\lambda_f = 2\pi/|F(\delta)|$, and the slower oscillation is the periodic variation of b with period close to $\lambda_s = 2\pi/|L(\delta)|$. The frequencies of these oscillations approach ω and Ω, respectively, as $h \to 0$. Figure 4a shows that the high frequency oscillations of a_+ are modulated by a slowly varying envelope, and the profile of b suggests a periodic behaviour with period $6\lambda_s$. These variations on slower time scales arise from nonlinear interactions between oscillating components in the solution, and their presence indicates that any analysis of the modulational behaviour must involve several time scales. Figure 4b shows that as ε increases from zero there is an increase in λ_s, and the modulations on the high frequency waves are more distinct. Figure 4c indicates that as ε is further increased there is side-band growth and an instability develops on a slow time scale. At $\varepsilon = 0$ the maximum value of $|a_+(t)|$ for $0 \leqslant t \leqslant 7.7$ is 0.99×10^{-4}, and at $\varepsilon = 6.5 \times 10^{-6}$ the maximum value of $|a_+(t)|$ in this interval is 0.013. The result of interest is that the introduction of a non-zero dispersion coefficient yields a semi-discrete system which permits modulational instabilities.

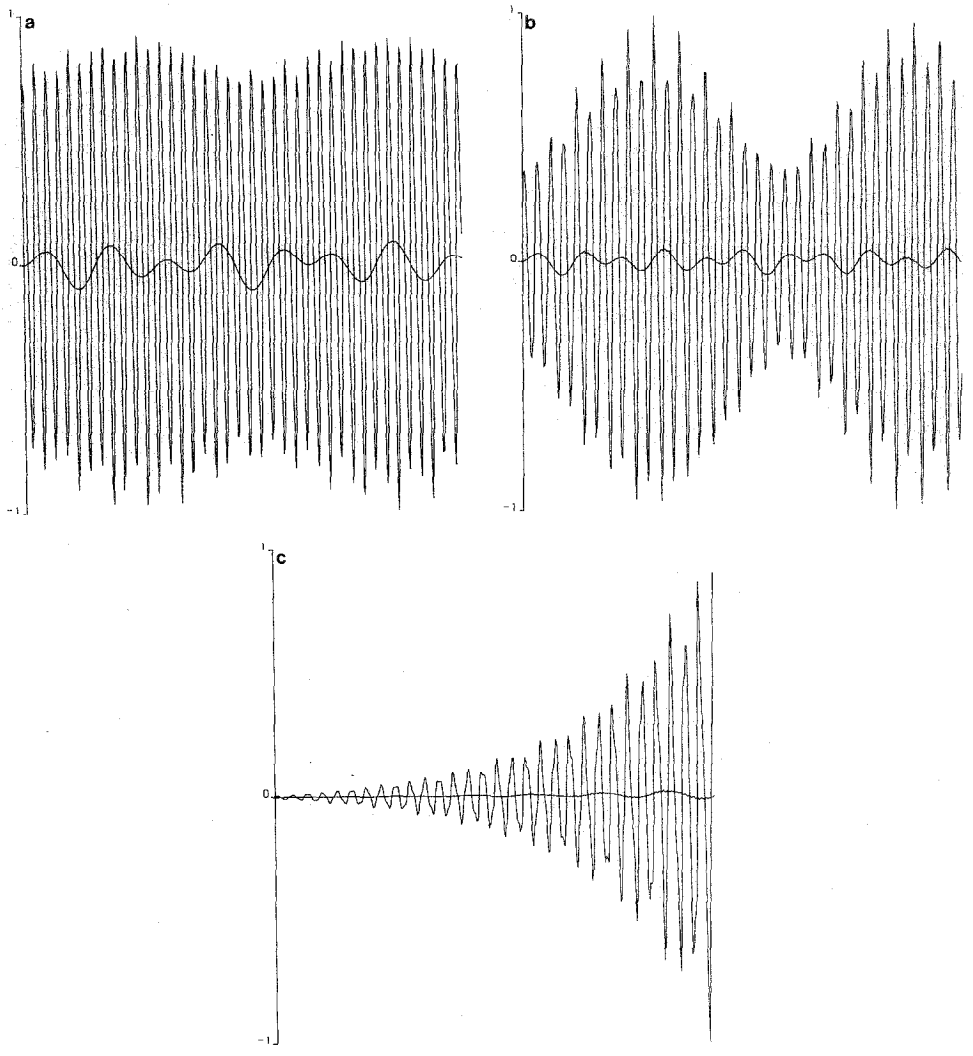

FIG. 4. Variation of real parts of a_+ and b with time given by the accurate solution of (3.2) and (2.10) with $E=0.2$, $J=120$, $\mu=3$, $U=0.6$ and $\theta=0$. (a)–(c) correspond to $\varepsilon=0$, 4.5 (-6), 6.5 (-6), and maximum times are 4.4, 6.3, and 7.7.

To examine the effect of variations in ε on the side-band growth for the fully discrete system we used a midpoint rule discretisation of (3.2), together with (2.11) and a time step given by $\gamma=k/h=1$. All parameters, except ε, were assigned as in the above semi-discrete calculations, and the same initial conditions were now imposed at time steps $n=0$, 1. Computed solutions using this scheme could equally be obtained by Fourier decomposition of appropriate leap-frog solutions of (2.2). Figures 5a, b, and c show the variations of the real parts of a_+ and b with time for

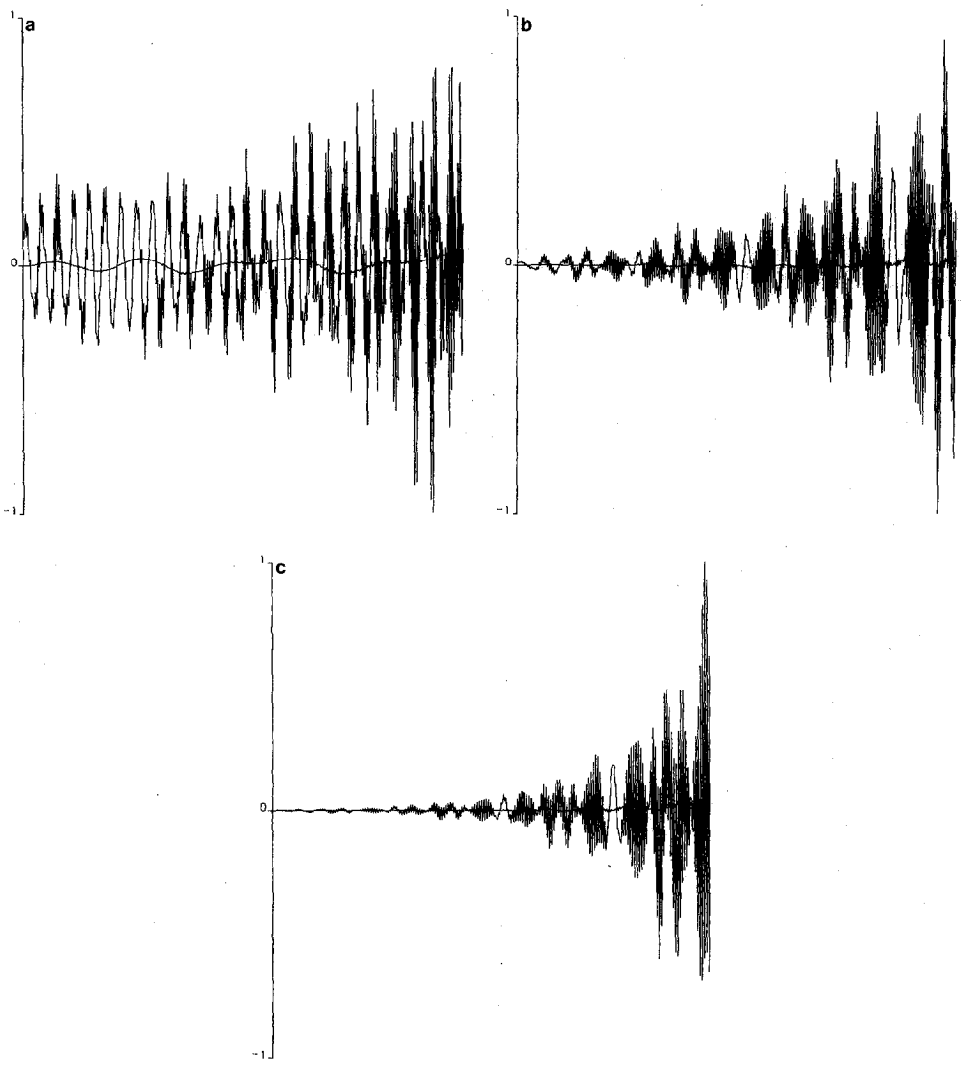

FIG. 5. Variation of real parts of a_+ and b with time given by the midpoint rule solution of (3.2) and (2.10) with $E=0.2$, $J=120$, $\mu=3$, $U=0.6$, $\theta=0$, and $\gamma=1$. (a)–(c) correspond to $\varepsilon=0$, 3.3 (-6), 3.4 (-6), and maximum time is 3.2 in each case.

$\varepsilon=0$, 3.3×10^{-6}, and 3.4×10^{-6}, respectively, and each figure covers the same time interval $0\leqslant t\leqslant 3.2$. The maximum values of $|a_+|$ over this range of integration are 0.50×10^{-3}, 0.65×10^{-2}, and 0.40×10^{-1} for the three values of ε, and these values indicate that the growth rate increases with ε. In the fully discrete system the introduction of ε has increased the strength of the modulational instability.

It is of interest to examine the effect of initial conditions on the side-band growth.

Accordingly, the calculation which produced Fig. 5a was repeated with a change only in the initial conditions at $t=k$. The solution of the linear part of (2.11) enables us to write $A(1)=A(0)\exp(-i\varphi)$, where φ is one of the values given by (2.6). The solution mode associated with the value $\varphi=\varphi_1$ is the principal mode and that associated with $\varphi=\varphi_2$ is a parasitic mode which arises from the two-step nature of the time discretisation. Figures 6a and b show the variations of the real parts of a_+ and b, with conditions at $t=k$ based on the principal and parasitic modes, respectively. As before, each figure is scaled and the time interval is $0\leqslant t\leqslant 3.2$. The figures show clearly that the growth rate is much stronger with the parasitic mode than with the principal mode. The result agrees with the analysis of Cloot and Herbst [3] who conclude that the parasitic mode is one of the primary sources of modulational instability in leap-frog discretisations of (1.1).

Cloot and Herbst [4] have recently analysed modulational instabilities of the KdV equation using an approach analogous to that which was previously applied to the inviscid Burgers equation [3]. Their analysis examines resonances introduced by the discretisations and it investigates conditions under which these resonances can give rise to instabilities. For example, they consider the semi-discrete system on the interval $[0, 2\pi]$ and they examine the stability of solutions of the form

$$U_j(t)=z[e^{i(kx_j-\omega_k t)}+(*)]+O(z^2), \qquad z\ll 1, \tag{3.5}$$

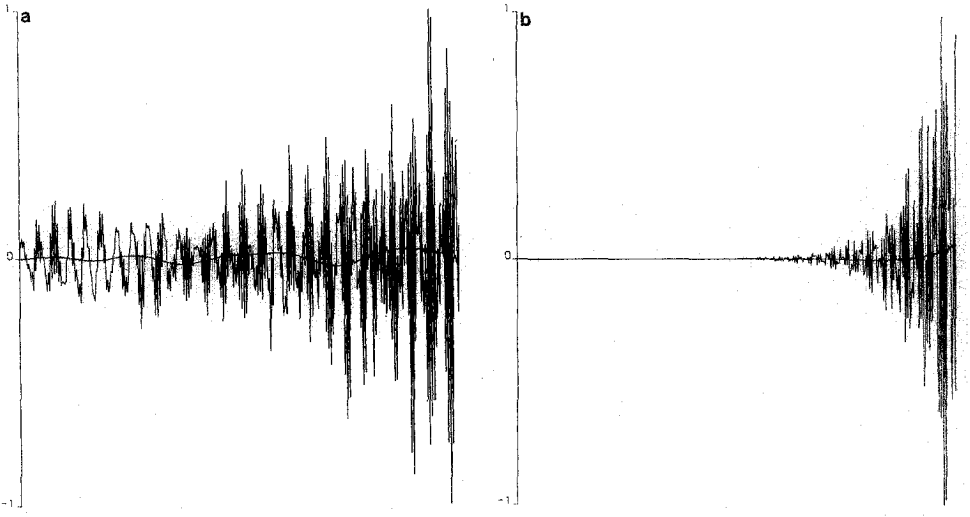

FIG. 6. Variation of real parts of a_+ and b with time given by the midpoint rule solution of (3.2) and (2.10) with $E=0.2$, $J=120$, $\mu=3$, $U=0.6$, $\theta=0$, $\gamma=1$, and $\varepsilon=0$. (a) and (b) correspond to principal and parasitic modes in initial conditions, and maximum time is 3.2 in each case.

where (*) denotes the complex conjugate and the frequency, ω_k, of mode k is given by the linearised dispersion relation

$$\omega_k = \frac{U}{H} \sin kH + \frac{(2\pi)^2 \varepsilon}{H^3} (\sin 2kH - 2 \sin kH). \tag{3.6}$$

Here $H = 2\pi h$, and this gives the mesh spacing on the interval $[0, 2\pi]$. They obtain, inter alia, conditions under which resonance between the modes $k+\mu$, $k-\mu$, and μ will give rise to instability: the analysis shows that side-band modes will grow, and instability will occur, if z exceeds a limiting value, z_{SB}. Details will be given in their forthcoming paper and to indicate the relevance to the present study it will suffice here to refer to results for $k = J/3$ and $\theta = 0$, when the three modes become those with coefficients a_+, a_-, and b in Eq. (3.4). For the data used to produce Fig. 4 it may be shown that z_{SB} decreases as ε increases through the values used in Figs. 4a, b, and c. This suggests that the semi-discrete system is destabilised to modulational instabilities as the dispersion coefficient, ε, increases from zero and it gives some support to the results presented here.

Cloot and Herbst [4] also show that additional resonance conditions also arise if the dispersion coefficient, ε, assumes certain values. At $k = J/3$, for example, one of these values is $\frac{1}{3}Uh^2$ which corresponds to the degeneracy of the stability triangle PQR as defined by (2.12). This additional resonance condition may be sufficient to induce side-band growth as ε approaches the value $\frac{1}{3}Uh^2$. Numerical results will be presented in [4] to show the possible destabilising effects of the dispersive term in the semi-discrete and fully discrete situations.

4. Leap-Frog Discretisation of (2.1)

The integrations described in the preceding section involved only those Fourier modes which are stimulated by first-order interactions between a basic 1-mode solution and a perturbed side-band mode. A solution of the complete partial difference equation (2.2) may contain all Fourier modes of the form $\exp(\pm 2\pi ijp/J)$, $j = 0, 1, ..., J$, where the mode number p is in the range $0 \leqslant p \leqslant J/2$. The 1-mode initial conditions for (2.2) at $t = 0$, k are given by (2.9) with $A(0) = A(1) = \sigma(1+i)$ and σ given by (2.13). To stimulate a side-band at mode number p we add

$$2c[\cos(2\pi jp/J) - \sin(2\pi jp/J)]$$

to node j, where $j = 0, 1, ..., J$ and c is a small positive number. As before, the stimulated mode is at $p = J/3 + \mu$.

Several observations were made by Sloan and Mitchell [7] concerning the growth of side-band modes for Burgers equation. It was noted, for example, that the modulation envelope is more distinct in some cases than in others, and in the preceding section of this paper it was pointed out that the clarity of the modulation is influenced by the spread of energy over additional modes. In this section it is of

interest to examine the effect of the dispersive term on the strength of side-band growth and on the spread of energy to other modes.

Equation (2.2) was integrated using the parameter values $E=0.2$, $J=120$, $\mu=3$, $U=0.6$, $\theta=0$, $\gamma=1$, $c=0.5\times10^{-4}$ with $\varepsilon=0$ and $\varepsilon=3.4\times10^{-6}$. This is the parameter set used in the side-band equations for the calculations displayed in Figs. 5a and c. Numerical results confirm that the initial growth rate of the instability is greater for the non-zero value of ε. This difference in growth rates continues as the instability develops, and at $n=220$ the magnitudes measured in the maximum norm $\|U^n\|_\infty=\max_j|U_j^n|$ are 0.12×10^2 and 0.19×10^4 for $\varepsilon=0$ and $\varepsilon=3.4\times10^{-6}$, respectively. The solution profiles, scaled so that $\|U^n\|_\infty=1$, are shown in Figs. 7a and b. The solutions appear to be approaching the forms $U_l=\kappa$, $U_{l+1}=-\kappa$, $U_j=0$ for $j\neq l$, $l+1$, where l is a positive integer and κ a real positive number. Vadillo and Sanz-Serna [8] have shown that this is the least stable solution of the leap-frog discretisation of the inviscid Burgers equation.

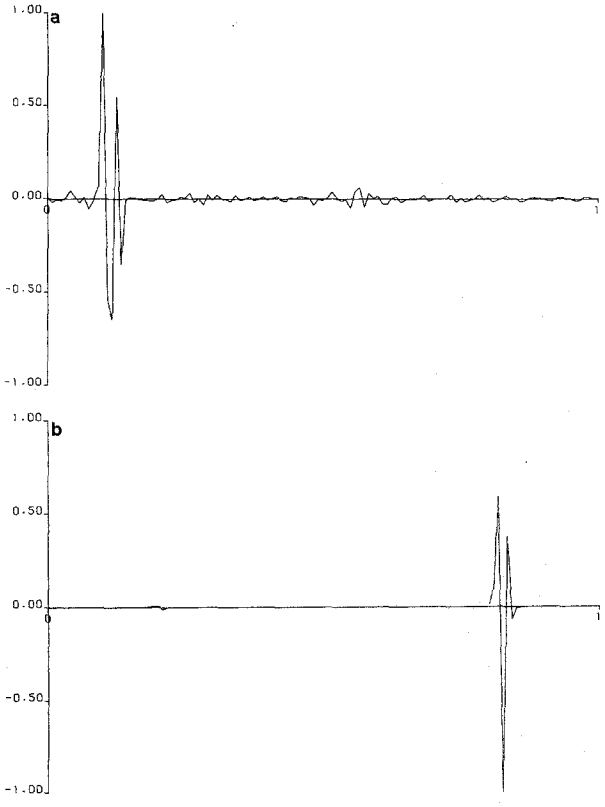

FIG. 7. Solution of (2.2) at step 220 with $E=0.2$, $J=120$, $\mu=3$, $U=0.6$, $\theta=0$, $\gamma=1$, and $c=0.5$ (-4). (a) and (b) correspond to $\varepsilon=0$ and $\varepsilon=3.4$ (-6).

At time step n in the solution of (2.2) the Fourier coefficient associated with mode p is

$$U(p, n)=\frac{1}{J}\sum_{j=0}^{J-1} U_j^n\, e^{-2\pi ijp/J}, \qquad -\frac{J}{2}<p\leqslant\frac{J}{2},$$

and the total energy, $\mathscr{E}(n)$, is given by

$$(\mathscr{E}(n))^2=(U(0, n))^2+\left(U\left(\frac{J}{2}, n\right)\right)^2+2\sum_{p=1}^{J/2-1}|U(p, n)|^2. \tag{4.1}$$

To measure the spread of energy brought about by second-order, nonlinear interactions we define the secondary energy, $\mathscr{E}_s(n)$, as in (4.1), with the summation restricted to modes not represented in (3.1). Equation (2.2) was integrated using the parameter values $E=0.2$, $J=120$, $\mu=3$, $\theta=0$, $\gamma=1$, $c=0.5\times 10^{-5}$. To measure the effect of variations of β on the spread of energy to secondary modes we computed the ratio $\mathscr{E}_s(n)/\mathscr{E}(n)$ for several values of α and β satisfying the constraint $\alpha-3\beta=0.9$. There was no evidence that the rate at which energy spreads to secondary modes is greatly influenced by the value of β. At $n=120$, for example, the above ratio has the values $0.29(-3)$, $0.43(-3)$, and $0.17(-3)$ for $\beta=0$, 0.01, and 0.02, respectively. Experiments performed with variations in θ and fixed valued of α and β indicate that energy spread to secondary modes is likely to be minimised at $\theta=\frac{2}{3}$.

5. Conclusions

Numerical experiments show how the results reported by Sloan and Mitchell [7] are modified by the introduction of dispersion. It was shown in Section 2 that the leap-frog scheme is stabilised to $3h$ perturbations about zero by the introduction of a positive dispersion coefficient, ε. One significant effect brought about by the dispersive term is that the semi-discrete system permits modulational instabilities. The observations by Sloan and Mitchell [7] and the analysis by Cloot and Herbst [3] indicate that such instabilities are not possible if $\varepsilon=0$.

Experiments on the fully discrete side-band equations suggest that the introduction of positive ε increases the strength of side-band growth. Numerical evidence is also presented to support the conclusion by Cloot and Herbst [3] that the parasitic mode is a primary source of modulational instability. Observations on solutions of the complete partial difference equations show that energy spread over Fourier modes is not significantly altered by the introduction of positive ε.

Acknowledgments

I am extremely grateful to Professor Ben Herbst for many useful discussions and for providing me with a preview of his joint paper with Dr. Alain Cloot on KdV modulational instabilities.

REFERENCES

1. T. B. BENJAMIN AND J. E. FEIR, *J. Fluid Mech.* **27**, 417 (1967).
2. W. L. BRIGGS, A. C. NEWELL, AND T. SARIE, *J. Comput. Phys.* **51**, 83 (1983).
3. A. H. J. CLOOT AND B. M. HERBST, *J. Comput. Phys.*, in press.
4. A. H. J. CLOOT AND B. M. HERBST, in preparation.
5. B. FORNBERG, *Math. Comp.* **27**, 45 (1973).
6. J. M. SANZ-SERNA, *J. Comput. Phys.* **47**, 199 (1982).
7. D. M. SLOAN AND A. R. MITCHELL, *J. Comput. Phys.* **67**, 372 (1986).
8. F. VADILLO AND J. M. SANZ-SERNA, *J. Comput. Phys.* **66**, 225 (1986).